NOTES AND CORRESPONDENCE

On the Sensitivity of Annular Mode Dynamics to Stratospheric Radiative Time Scales

ANDREW J. CHARLTON-PEREZ AND ALAN O'NEILL

Department of Meteorology, University of Reading, Reading, United Kingdom

(Manuscript received 19 December 2008, in final form 26 May 2009)

ABSTRACT

Long decorrelation time scales of the annular mode are observed in the lower stratosphere. This study uses a simple dynamical model, which has been used extensively to study stratosphere–troposphere coupling to investigate the origin of the long dynamical time scales. Several long runs of the model are completed, with different imposed thermal damping time scales in the stratosphere. The dynamical time scales of the annular mode are found to be largely insensitive to the input thermal damping time scales, producing similar dynamical time scales in all cases below 50 hPa. This result suggests that the hypothesis that long time scales in the lower stratosphere are due to long radiative time scales in this region is false.

1. Introduction and motivation

Predictability of the tropospheric circulation, on time scales longer than that of individual weather systems, can arise due to the presence of a slowly evolving boundary condition, which imparts significant predictability on the tropospheric flow (Palmer and Anderson 1994). This principle has long been established for predictable changes to the ocean circulation in the tropics, such as El Niño–Southern Oscillation (ENSO). More recently, attention has begun to be paid to other potential sources of predictability for the atmosphere. Particularly in the extratropics, other slowly evolving regions of the earth system, such as fall snow extent (Cohen and Fletcher 2007), soil moisture (Douville 2003), and the wintertime lower-stratospheric state (Baldwin and Dunkerton 2001), have been shown to have some effect on tropospheric conditions beyond the 10-day predictability range of tropospheric weather.

This study investigates the origin of slowly varying circulations in the wintertime lower stratosphere and their impact on tropospheric variability in a simple model of the stratosphere–troposphere system based on that of Polvani and Kushner (2002). The hypothesis that long dynamical time scales in the lower stratosphere are simply a consequence of the long, local radiative time scales is tested. Radiative relaxation time scales are very long in the lower stratosphere (around 40 days at 100 hPa in midwinter) and very fast in the upper stratosphere [around 5 days at 1 hPa; see Newman and Rosenfield (1997)]. An alternative hypothesis is that the long, local dynamical time scales are a result of coupled dynamical variability acting over the depth of the extratropical stratosphere. A very simple example of this idea is demonstrated in the paper by Barsugli and Battisti (1998). Here, when two red-noise processes are coupled together, the resulting autocorrelation of both processes is increased above their local damping time scales. Although the study of Barsugli and Battisti (1998) refers to the atmosphere and ocean, a similar model could be imagined for the stratosphere with a region of long radiative time scales in the lower stratosphere and short radiative time scales in the upper stratosphere. In this very simple model, coupling between the two regions is essential to increasing the autocorrelative time scales of both regions.

The primary focus of the study is on the behavior of the annular mode (Thompson and Wallace 2000) in the wintertime lower-most stratosphere between 100 and 300 hPa. Decorrelation time scales for the annular mode in this region are estimate to be 30 days (Baldwin et al. 2003, their Fig. 1). Variability in the annular mode in this region has a high correlation with the troposphere (Baldwin

Corresponding author address: Andrew J. Charlton-Perez, P.O. Box 243, Department of Meteorology, University of Reading, Reading, Berkshire, RG6 6BB, United Kingdom.
E-mail: a.j.charlton@reading.ac.uk

DOI: 10.1175/2009JCLI2995.1

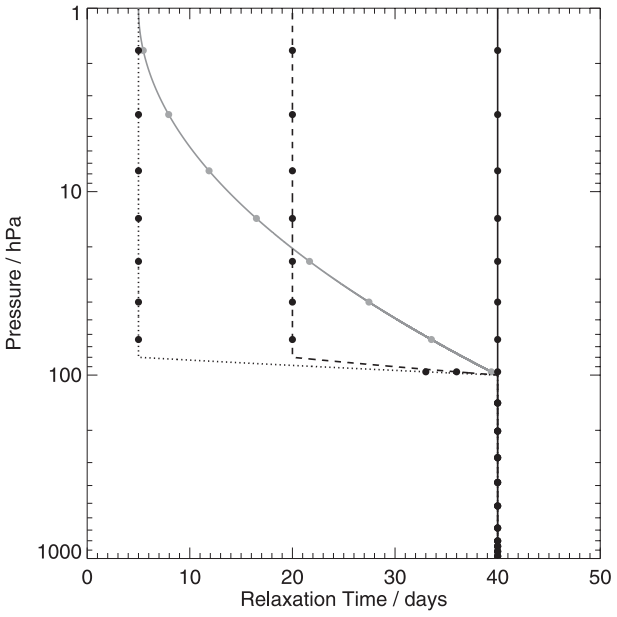

FIG. 1. Input value of thermal relaxation time scale outside the tropics for four initial integrations as a function of pressure. Dots show the position of model levels. Slow case (solid line), midcase (dashed line), fast case (dotted line), and real case (gray line) are shown.

et al. 2003; Charlton et al. 2003). To make optimal use of the lower stratosphere for seasonal prediction it is important to understand what causes the long dynamical time scales in this region, and what impacts the long time scales have on tropospheric variability. Some studies have suggested that the persistence of anomalies in the tropospheric annular mode following stratospheric sudden warmings is due to long-lasting diabatic heating anomalies in the lower stratosphere (Thompson et al. 2007). In this sense it is necessary to understand the reasons for the persistence of anomalies in the lower stratosphere if progress is to be made on understanding coupling between the stratosphere and troposphere. The manuscript is structured in the following way: The model setup and experimental design are described in section 2; section 3 describes the model climatology and variability. Section 4 describes how dynamical time scales are calculated and section 5 shows the main results of the study. Section 6 presents a summary and conclusions.

2. Model setup and experimental design

Model setup

We use the Reading, United Kingdom, intermediate general circulation model (IGCM) in its dynamical core mode. The model is based on the spectral dynamical core of Hoskins and Simmons (1975) and is used in this study in a similar simplified dynamical format to that of James and James (1992). The model is run with a horizontal truncation of T42, with 20 levels in the vertical and a model top at 0.08 hPa. The model uses an identical set of physical parameterizations as those used by Polvani and Kushner (2002; note, we were aware of, and made use of the corrigendum to this paper) to produce a simplified version of the stratosphere–troposphere system. Model physics are represented by Rayleigh friction at the top and bottom of the model and Newtonian cooling throughout the model domain, both of which are calculated in gridpoint space.

Key parts of the model setup are the equilibrium temperature profile $T_{\rm eq}$ and the time scale for relaxation to this profile. The equilibrium temperature profile is identical to that of Polvani and Kushner (2002), as identified in their appendix, and uses identical parameters. Polvani and Kushner vary the state of the stratosphere in their model by changing the value of a parameter γ, which changes the size of the equilibrium, stratospheric, pole-to-equator temperature gradient. In our experiments, this value is set to 1 K km^{-1}. As in Polvani and Kushner, horizontal gradients in equilibrium temperature are imposed in the Southern Hemisphere of the model only, and all experimental analysis is done there. The position of the tropospheric jet is shifted equatorward in the Southern Hemisphere compared to the Held and Suarez (1994) forcing scheme, using an additional term in the $T_{\rm eq}$ profile below 100 hPa as in Polvani and Kushner [their Eq. (A4)].

Our experiments examine the response of the large-scale variability to changes to the rate at which temperatures relax toward the equilibrium temperature profile $T_{\rm eq}$. We define thermal relaxation rates τ, which vary in the troposphere and stratosphere as

$$\tau(p, \phi) = \begin{cases} \tau_T(\sigma, \phi) & \text{for } \sigma \geq \sigma_T; \\ \tau_S(\sigma, \phi) & \text{for } \sigma \geq \sigma_T; \end{cases}$$

where $\sigma_T = 0.1$.

In the troposphere,

$$\tau_T = \tau_a + (\tau_s - \tau_a) \max\left(0, \frac{\sigma - \sigma_b}{1 - \sigma_b}\right) \cos^4\phi,$$

where $\tau_a = 1/40$ day^{-1}, $\tau_s = 1/4$ day^{-1}, $\sigma_b = 0.7$, and ϕ is latitude.

In the stratosphere four different profiles of thermal relaxation rate are used. The ''fast,'' ''mid-'' and ''slow'' profiles are defined by the formula

$$\tau_S = \tau_{\rm str} + (\tau_a - \tau_{\rm str}) \max\left(0, \frac{\sigma - \sigma_{\rm str}}{1 - \sigma_{\rm str}}\right),$$

where $\tau_a = 1/40$ day^{-1}, $\sigma_{str} = 0.08$, and $\tau_{str} = 1/5$, $1/20$, and $1/40$ day^{-1} for the fast, mid-, and slow profiles, respectively.

Additionally, the ''real'' thermal relaxation rate is defined as

$$\tau_S = \left(5 - \left\{\frac{5-40}{4}[\log_{10}(1000\sigma)]^2\right\}\right)^{-1},$$

which represents a smooth transition between relaxation rates of 40 days near the tropopause to 5 days at the stratopause.

The resulting four thermal relaxation rate profiles are shown in Fig. 1, for a latitude outside the tropics. The slow profile, shown in the solid line, is identical to that used by Polvani and Kushner (2002). The real profile, shown in the gray line, is an approximation to the thermal relaxation rates in the real atmosphere as calculated by Newman and Rosenfield (1997).

In the first set of integrations, simplified orography is also included in the model. This has the functional form (units of the equation are meters) of

$$Z_{surf} = 2500e\frac{-(\phi-35)^2}{625}\left[e\frac{-(\lambda-90)^2}{100} + e\frac{-(\lambda-270)^2}{100}\right].$$

In all cases the model is integrated for 10 000 days, with no change to the equilibrium temperatures, and hence no seasonality. The first 800 days of each model is assumed to be model spinup and is discarded. Analysis is performed on the final 9200 days. Two sets of experiments are described here. The first set examines the impact of changing thermal relaxation rates on the model dynamics with the orography included and is referred to as the ''orog'' runs. The second set of experiments is identical to the first, but with a flat bottom boundary, and it is referred to as the ''no orog'' runs.

Our primary means of analysis of the results is through estimation of the *e*-folding time scale of the model's annular mode. We follow the methodology of Gerber et al. (2008) to determine the structure of the annular mode, estimate its *e*-folding time scale, and add error estimates. The convention of Baldwin et al. (2003) is used to describe the annular mode: AO is used for the surface signature of the annular mode calculated using mean sea level pressure, and AM is used for the signature of the mode elsewhere calculated using geopotential height. In both cases, the daily amplitude of the mode is referred to as the Annular Mode Index (AMI). As other authors have recently stated, there are significant issues that must be dealt with when diagnosing the time scale of our model (Gerber et al. 2008; Chan and Plumb 2009). In particular, models of the Polvani and Kushner (2002) type (with some sets of parameter choices) have an unrealistic ''switching'' behavior, in which the tropospheric jet tends to persist in one mean location for thousands of days before switching to another location. These issues are explicitly discussed in section 4.

3. Model climatology and variability

Before discussing changes to the model's annular mode as a result of input changes in the thermal relaxation time scale, the impact of these changes on the model's mean climate and variability is first examined. Figure 2 shows the zonal mean zonal wind and its standard deviation plotted for the final 9200 days of each integration, with idealized orography included. As in other implementations of the Polvani and Kushner (2002) forcing, the model produces a somewhat realistic climatology of the zonal mean zonal wind, with a strong westerly stratospheric jet located around 60°S. In the troposphere, a subtropical jet of approximately the correct magnitude and spatial scale is produced, located near to 30°N/S. The zonal mean zonal wind produced by our model, with a completely different dynamical core to that used by Polvani and Kushner, is almost identical to that shown in Polvani and Kushner (2002). A useful comparison can be made between Fig. 1b of Polvani and Kushner and our slow case in Figs. 2 and 3.

Comparison between the four cases in Fig. 2 shows that the effect of changing the radiative relaxation rate in the stratosphere is to cause a marked increase in the strength of the jet in the upper stratosphere. As the radiative time scale becomes shorter, the strength of the jet approaches that which would be predicted by the thermal wind balance from the T_{eq} profile. Experiments with stronger jets in the middle stratosphere (fast and mid-), also produce tropospheric jets that are slightly displaced toward the pole. The correlation between stratospheric jet strength and the location of the tropospheric jet has previously been noted in models of this kind (Polvani and Kushner 2002). The strength of the jet in each case is well correlated with the standard deviation of the zonal mean zonal wind in the upper stratosphere. Experiments with weaker relaxation in the upper stratosphere experience much larger amounts of zonal wind variability. In the troposphere, zonal mean zonal wind variability is concentrated on the flanks of the subtropical jet, a key part of the annular mode variability, which is discussed in the following two sections.

The mean climatology and variability of the experiments without orography are very similar to those with orography (Fig. 3). Runs without orography have a reduced amplitude of planetary Rossby waves. As a consequence of the reduction in the strength of planetary waves, the strength of both the tropospheric and stratospheric jets

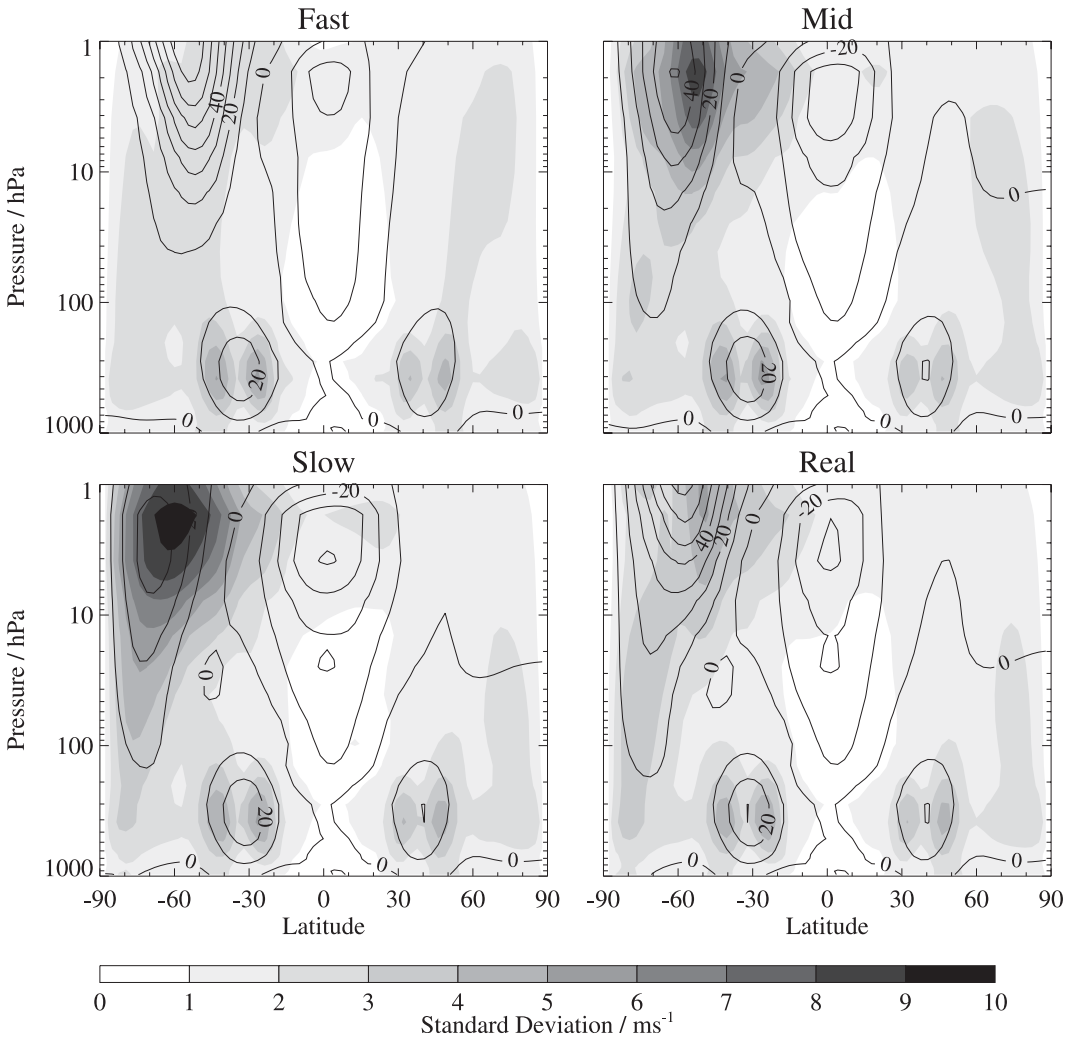

FIG. 2. Zonal mean zonal wind (contours) and its standard deviation (shading) for the final 9200 days of each run in the integrations with idealized orography. Contour interval for zonal mean zonal wind is 10 ms^{-1}.

in the cases without orography is increased. Similarly, the variability of the zonal winds in the upper stratosphere is also somewhat reduced in the runs without orography.

The stratospheric and tropospheric climatology produced by the IGCM generally compares favorably with that produced by other models run with the Polvani and Kushner (2002) forcing setup (e.g., Chan and Plumb 2009). Although the climate produced by the model is a simplification of the real atmospheric circulation, its similarity allows us to conduct useful experiments to try to understand the physical processes involved in setting the time scale of the annular mode.

4. Diagnosing annular mode time scales

To test the hypothesis that long dynamical time scales in the lower stratosphere are simply a consequence of the long local radiative time scales, it is necessary to develop a method for comparing dynamical time scales between experiments. In this section we discuss the methods adopted in the present study; it is not suggested that these would be suitable for all applications.

There has been a great deal of recent interest in establishing the best methodology to characterize the time scale of annular modes in models and reanalysis data (e.g., Gerber et al. 2008; Keeley et al. 2009). A particular focus has been the extent to which calculated time scales for the annular mode describe its observed behavior and decorrelative properties. This study is focused on understanding the processes that control the observed day-to-day synoptic variability of the annular mode. As such, very low-frequency oscillations of the annular mode index, which may change the structure of its autocorrelation function, are considered to be

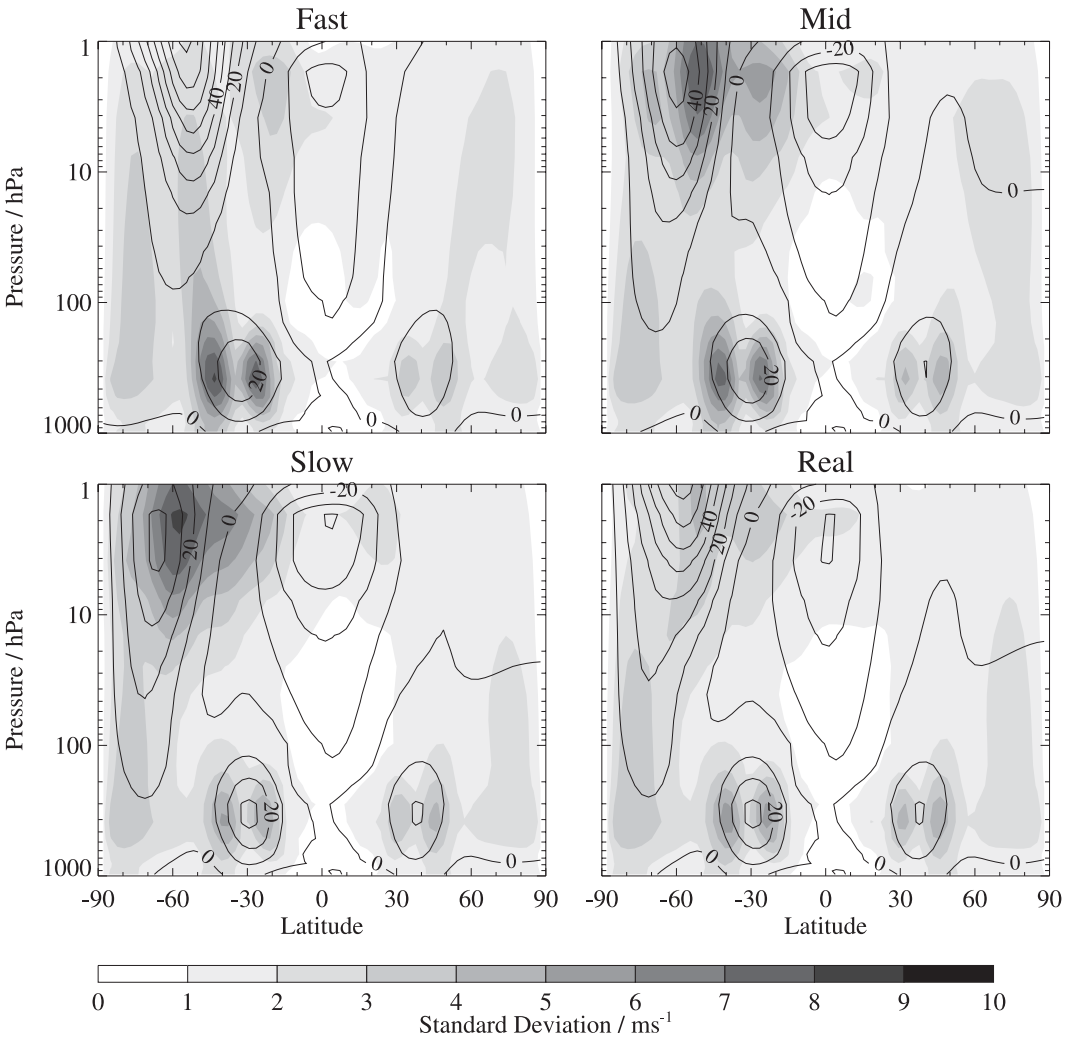

FIG. 3. Zonal mean zonal wind (contours) and its standard deviation (shading) for the final 9200 days of each run in the integrations without orography. Contour interval for zonal mean zonal wind is 10 ms^{-1}.

problematic. In models of the Polvani and Kushner (2002) type, low-frequency oscillations in the position of the jet are known to exist (Chan and Plumb 2009) for some sets of parameter choices. These low-frequency oscillations are unrealistic and are partly a product of the lack of seasonality in the model. Initial analysis of raw AMI data showed that it is very easy to draw erroneous conclusions about the behavior of the annular mode in the model if these low-frequency oscillations are not removed.

To demonstrate this point the following analysis is presented, which compares the autocorrelative behavior of the raw AMI series with a series that has been high-pass filtered to remove components with periods of 400 days and greater. The filter used is a simple running mean smoother,

$$\mathrm{AMI}_{\mathrm{high}} = \mathrm{AMI} - \mathrm{AMI}_{\mathrm{low}}, \tag{1}$$

where $\mathrm{AMI}_{\mathrm{low}}$ is a centered, boxcar running mean with 401 elements. This very simple filter is chosen because it illustrates the impact of low-frequency variability on the time scale of the AMI.

Figure 4 shows a comparison between the autocorrelation function of the raw and filtered AMI data for an arbitrarily selected run of the model (in this case the integration with orography included and the slow radiative time-scale profile). The autocorrelation function of the raw AMI data, shown by the gray line, deviates strongly from the exponential form expected for a red-noise or AR1 process (Wilks 1995). The autocorrelation remains close to or above the value $1/e$ beyond 30 days. An e-folding time scale for the autocorrelation function

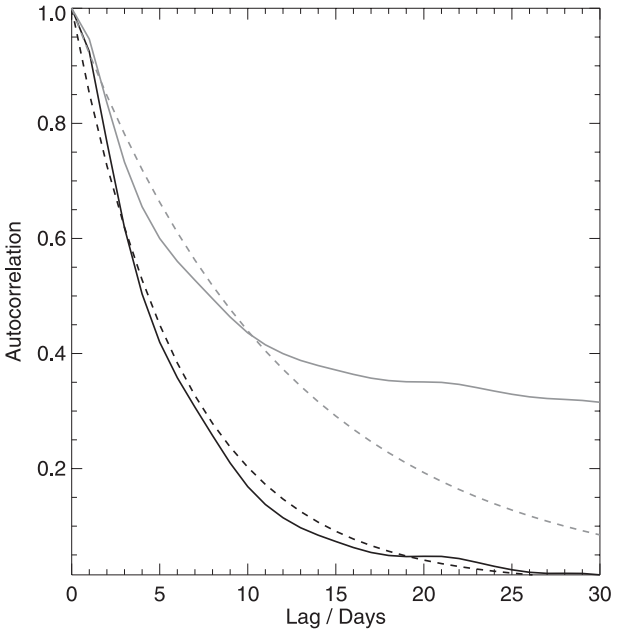

FIG. 4. Autocorrelation of the AMI for the first EOF of sea level pressure for the experiment with idealized orography and the slow relaxation rate profile. The autocorrelation calculated with the raw AMI data (gray solid line), autocorrelation calculated with the raw AMI data (gray dashed line), and autocorrelation for AMI data that has been high-pass filtered to remove variability at periods longer than 400 days (black solid line, see text for details). An exponential fit to the filtered AMI data (black dashed line) is also shown.

can be estimated by fitting an exponential function to the observed autocorrelation function between lag zero and the point at which the time series drops below the value 1/*e* (Gerber et al. 2008). Using this procedure, a time scale of 12 days is estimated for the raw AMI data. In comparison, the autocorrelation function of the high-pass-filtered version of the same time series (shown in the black line) is much closer to the exponential form. The autocorrelation at lags beyond 15 days is much reduced in comparison to the raw AMI time series, suggesting that much of the autocorrelation in the raw time series is due to the persistent, unrealistic low-frequency variability. The estimated time scale for the filtered AMI time series is 6 days, a large reduction in comparison to the raw AMI time series. It is also important to note however, that at longer lags the exponential fit to the autocorrelation is not particularly effective in either the filtered or unfiltered cases. The aim of the filtering procedure is to improve the fit at the shorter lags (note that information beyond 1/*e* is ignored) only, because it is these time scales that are of most interest for the annular mode dynamics investigated in this study.

The aliasing of low-frequency variability onto mid-range time scales in the autocorrelation function means that making an estimate of the true time scale of the annular mode in the model AMI data series is extremely difficult and is beset by problems of nonstationarity. Figure 5 shows estimates of the time scale and mean of the AMI at 300 hPa for the same integration. Gray symbols show estimates for the raw AMI time series and black symbols indicate estimates for the high-pass-filtered AMI time series. Estimates of the annular mode time scale for each 1000-day part of the time series show variations of the same order of magnitude as the estimated time scale itself. This high degree of nonstationarity means that a stable estimate of the time scale is hard to achieve and can easily be altered by considering different parts of the same run. The nonstationarity of the

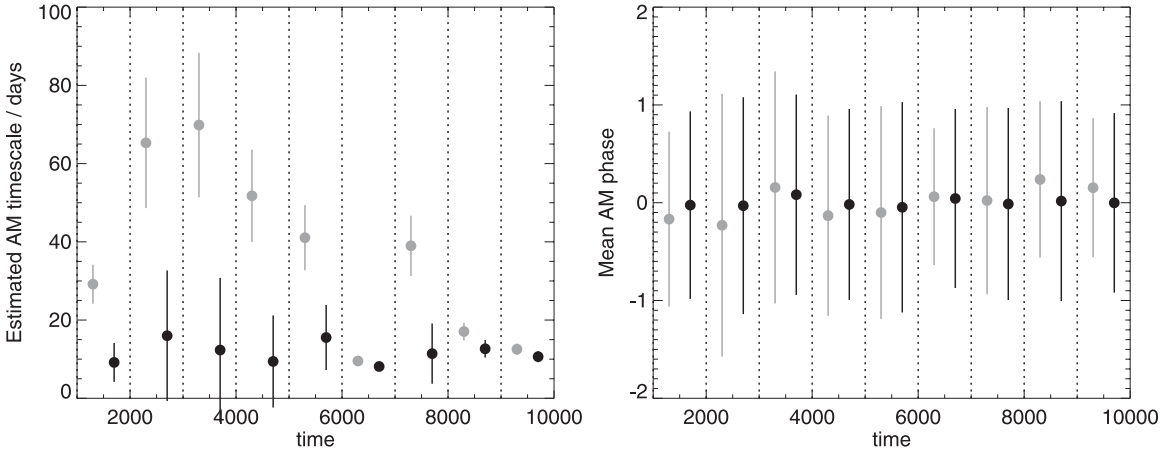

FIG. 5. Estimates of (left) AM time scale and (right) AM mean for independent 1000-day sections of the integration with idealized orography and the slow radiative cooling time scale on the 300-hPa pressure surface. Results from calculations made with the raw AMI data (gray dots), and calculations made with a high-pass-filtered version of the AMI data that have variability at periods longer than 400 days removed (black dots). Symbols in the lhs have error bars on each estimate based on the formulation of Gerber et al. (2008, see text for details), symbols on the rhs have error bars plotted at one standard deviation for each 1000-day block. Note that symbols have been offset in time for ease of viewing.

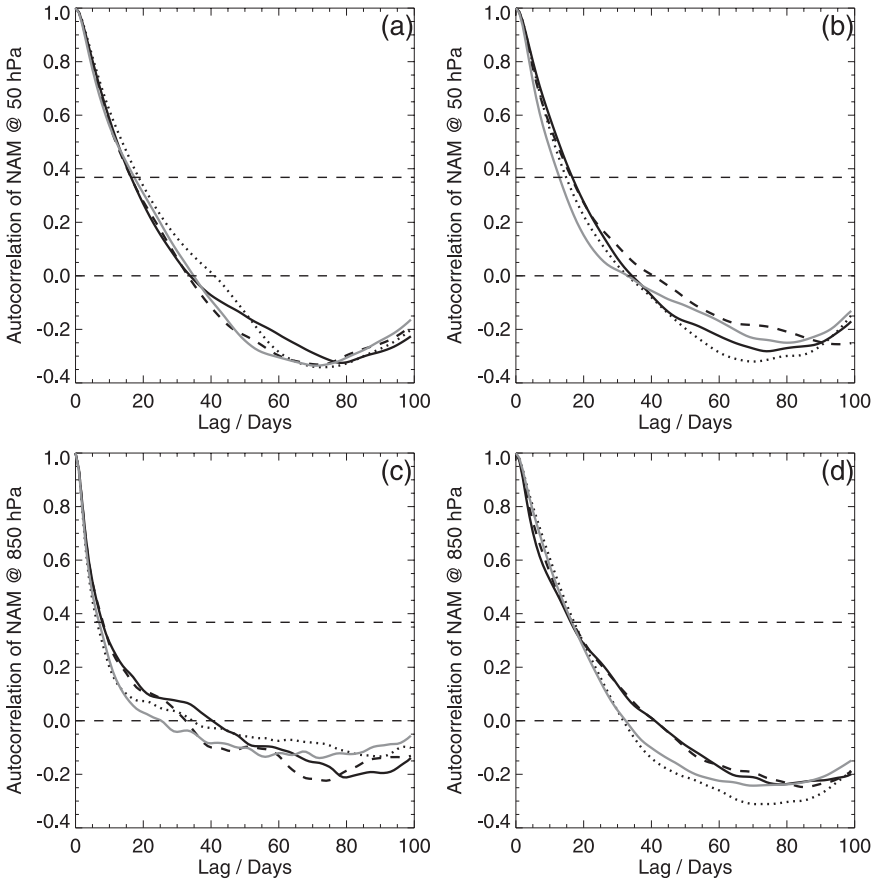

FIG. 6. Autocorrelation function of high-pass-filtered AM index time series. Line convention in all four panels is the same; runs with fast radiative time scale profile (solid black), runs with midradiative time scale profile (dashed black), runs with slow radiative time scale profile (dotted black), and runs with real radiative time scale profile (solid gray) are shown. Panels show results from runs with idealized orography at (a) 50 and (c) 850 hPa and without orography at (b) 50 and (d) 850 hPa. Horizontal dashed lines show the position of the zero and 1/*e* autocorrelation points.

raw AMI time series is emphasized by the large changes to the AMI mean for different 1000-day parts of the time series (Fig. 5b). In contrast, the high-pass-filtered time series shows little evidence of nonstationarity and allows a stable estimate of the time scale to be made.

Therefore, in the following analysis, the autocorrelative properties of the annular mode in our experiments are compared using filtered AMI time series. The same 401-element boxcar filter used in this section is also used in the following analysis. This filtering strategy is crude, and the choice of filter and its length is arbitrary. It is adopted so that the procedure is reproducible and it allows us to draw out key differences and similarities between our experiments. We explored the sensitivity of the results to the choice of filter length. While the absolute values of *e*-folding time scale are sensitive to the choice of filter length, the broad, qualitative conclusions drawn from the analysis are robust for other filter lengths.

5. The impact of changing stratospheric radiative time scales

To test the hypothesis posed in the introduction to the paper, the autocorrelative properties of the annular mode are compared across the eight model integrations. Figure 6 shows the autocorrelation function at 50 and 850 hPa for the sets of model integrations with and without idealized orography. Differences in the properties of the autocorrelation function of the high-pass-filtered AMI data are very small both in the troposphere and in the stratosphere.

The decay of the autocorrelation function at 50 hPa is similar in the cases with and without orography and

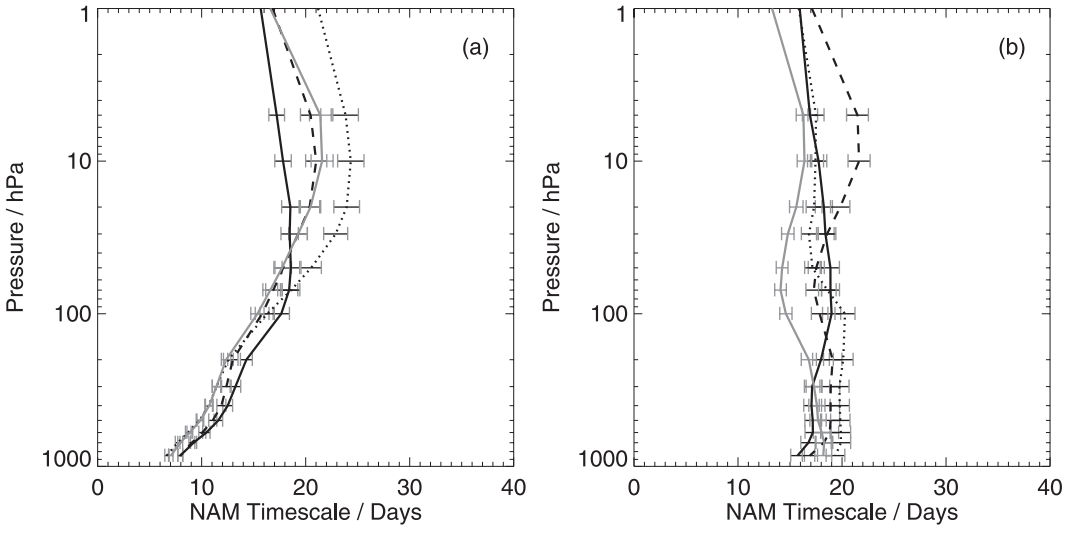

FIG. 7. *E*-folding time scale of the filtered AM index time series as a function of pressure for cases (a) with idealized orography and (b) without orography. Line convention is as in previous plots, runs with fast radiative time-scale profile (solid black), runs with midradiative time scale profile (dashed black), runs with slow radiative time scale profile (dotted black), and runs with real radiative time scale profile (solid gray) are shown. Error estimates for the time scale are shown with thin horizontal bars following the procedure of Gerber et al. (2008), see text for details.

appears unrelated to the input radiative time scale. This suggests that the time scale of variability in the stratosphere is unrelated to the input radiative time scale of the model. It is important to point out that the absolute amplitude of variability is dependent on the input time scale and the presence of orography; cases with stronger damping generally have reduced variability.

At 850 hPa, there are large differences in the decay of the autocorrelation function between the cases with and without idealized orography, but little sensitivity to the input stratospheric radiative damping rate. The reduction of the time scale of the annular mode when orography and planetary waves are present is well known (Gerber et al. 2008). The presence of planetary waves is thought to lead to a change in the transient eddy interaction with the tropospheric jet.

Finally, the calculated time scale of the annular mode as a function of pressure is shown in Fig. 7. The profile of dynamical time scales in the experiments without orography is shown in Fig. 7a, and generally has the form that is expected with short dynamical time scales in the troposphere, rising to longer time scales in the stratosphere. Below 50 hPa, there are very few parts of the profile over which there are large and significant differences between the dynamical time scales in the four runs. Even in cases where runs have significant differences according to the error bars, the magnitude of differences between the dynamical time scales estimated for the four runs is very small. In the middle and upper stratosphere, dynamical time scales appear to be most strongly influenced by the input radiative time scales. For example, at 10 hPa the fast run has the shortest dynamical time scales followed by the mid- and slow runs. The real radiative time scale run exhibits dynamical time scales very close to those of the midrun.

For the runs without imposed orography, Fig. 7b, a more complex profile of dynamical time scales is apparent. Below 200 hPa, dynamical time scales in the four models are virtually indistinguishable. Between 50 and 100 hPa, the fast, mid-, and slow radiative time scale runs also have very similar dynamical time scales, but the real run has slower time scales, with a significant and moderately large difference from the rest of the integrations. Above 50 hPa, there are less clear and predictable distinctions between the four runs without orography than those with orography shown in Fig. 7a.

In summary, Fig. 7 confirms results shown in Fig. 6; there is little dependence of the annular mode time scale below 50 hPa, the lower stratosphere, and the troposphere on the input radiative damping time scale.

6. Discussion and conclusions

The experiments reported in this short investigation use a flexible model introduced by Polvani and Kushner (2002) to investigate the decorrelative behavior of the annular mode. The autocorrelation function of the annular mode is compared for sets of experiments that vary principally in their imposed stratospheric thermal

relaxation rate. The experiments are designed to test the hypothesis that long dynamical time scales in the lower stratosphere are simply a consequence of the long, local radiative time scales in the same region. In our experiments, changing the input stratospheric radiative damping rate had very small, and rarely significant, impacts on the annular mode time scale in the troposphere and lower stratosphere.

An obvious distinction between the dynamical time scales estimated in the present study and those published for reanalysis data in the literature (e.g., Baldwin et al. 2003) is that the long decorrelation time scales in the lower stratosphere, of the order 40 days, are not present in the IGCM. As is evident in our study, and has been discussed in recent papers (e.g., Keeley et al. 2009), estimating a single, definitive time scale for the annular mode autocorrelation function is extremely difficult. A particular difficulty arises because of the modulation of annular mode variance by the seasonal cycle (S. Osprey 2009, personal communication). We hypothesize that the differences between the 20-day time scale for the lower stratosphere estimated here and the 40-day time scale typically shown for reanalysis data may simply be a consequence of differences in methodology, and that the Polvani and Kushner (2002) model setup adequately represents the physical processes at work in the stratosphere and troposphere on these large scales.

It is also important to emphasize, however, that our results do not imply that the long dynamical time scales observed in the tropospheric annular mode in midwinter are unrelated to the long *dynamical* time scales in the stratospheric annular mode. A robust influence of stratospheric variability on the behavior and time scale of the tropospheric jet is described in detail in Gerber and Polvani (2009). Rather, the results of the present study emphasize the point made by Gerber and Polvani (2009) that climate models that lack a full description of stratospheric dynamics are likely to have significant biases in their extratropical mean climate and variability. A model with a correct treatment of stratospheric radiative processes but incorrect stratospheric variability is both possible and undesirable.

Acknowledgments. The authors wish to thank Paul Kushner, Ed Gerber, Scott Osprey, and the stratosphere and climate group at the University of Reading for productive discussions. AJC-P is funded by a NERC Postdoctoral Fellowship, Reference NE/C518206/1.

REFERENCES

Baldwin, M. P., and T. J. Dunkerton, 2001: Stratospheric harbingers of anomalous weather regimes. *Science,* **244,** 581–584.

——, D. B. Stephenson, D. W. J. Thompson, T. J. Dunkerton, A. J. Charlton, and A. O'Neill, 2003: Stratospheric memory and extended-range weather forecasts. *Science,* **301,** 636–640.

Barsugli, J. J., and D. S. Battisti, 1998: The basic effects of atmosphere–ocean thermal coupling on midlatitude variability. *J. Atmos. Sci.,* **55,** 477–493.

Chan, C. J., and R. A. Plumb, 2009: The response to stratospheric forcing and its dependence on the state of the troposphere. *J. Atmos. Sci.,* **66,** 2107–2115.

Charlton, A. J., A. O'Neill, D. B. Stephenson, W. A. Lahoz, and M. P. Baldwin, 2003: Can knowledge of the state of the stratosphere be used to improve statistical forecasts of the troposphere? *Quart J. Roy. Meteor. Soc.,* **129,** 3205–3225.

Cohen, J., and C. Fletcher, 2007: Improved skill of Northern Hemisphere winter surface temperature predictions based on land–atmosphere fall anomalies. *J. Climate,* **20,** 4118–4132.

Douville, H., 2003: Assesing the influence of soil moisture on seasonal climate variability with AGCMs. *J. Hydrometeor.,* **4,** 1044–1066.

Gerber, E. P., and L. M. Polvani, 2009: Stratosphere–troposphere coupling in a relatively simple AGCM: The importance of stratospheric variability. *J. Climate,* **22,** 1920–1933.

——, S. Voronin, and L. M. Polvani, 2008: Testing the annular mode autocorrelation timescale in simple atmospheric general circulation models. *Mon. Wea. Rev.,* **136,** 1523–1536.

Held, I. M., and M. J. Suarez, 1994: A proposal for the intercomparison of dynamical cores of general circulation models. *Bull. Amer. Meteor. Soc.,* **75,** 1825–1830.

Hoskins, B. J., and A. J. Simmons, 1975: A multi-layer spectral model and the semi-implicit method. *Quart. J. Roy. Meteor. Soc.,* **101,** 637–655.

James, I. N., and P. M. James, 1992: Spatial structure of ultra-low-frequency variability of the flow in a simple atmospheric circulation model. *Quart. J. Roy. Meteor. Soc.,* **118,** 1211–1233.

Keeley, S. P. E., R. Sutton, and L. Shaffrey, 2009: On the autocorrelation of the North Atlantic oscillation. *Geophys. Res. Lett.,* in press.

Newman, P. A., and J. E. Rosenfield, 1997: Stratospheric thermal damping times. *Geophys. Res. Lett.,* **24,** 433–436.

Palmer, T. N., and D. L. T. Anderson, 1994: The prospects for seasonal forecasting–a review paper. *Quart. J. Roy. Meteor. Soc.,* **120,** 755–793.

Polvani, L. M., and P. J. Kushner, 2002: Tropospheric response to stratospheric perturbations in a relatively simple general circulation model. *Geophys. Res. Lett.,* **29,** 1114, doi:10.1029/2001GL014284.

Thompson, D. W. J., and J. M. Wallace, 2000: Annular modes in the extratropical circulation. Part I: Month-to-month variability. *J. Climate,* **13,** 1000–1016.

——, J. C. Furtado, and T. G. Shepherd, 2007: On the tropospheric response to anomalous stratospheric wave drag and radiative heating. *J. Atmos. Sci.,* **63,** 3315–3332.

Wilks, D. S., 1995: *Statistical Methods in the Atmospheric Sciences*. Academic Press, 467 pp.